GeoPlaNet

Co-funded by the ERASMUS + Programme of the European Union

DIPARTIMENTO DI GEOSCIENZE

UNIVERSITAS STUDII PADUANI

IRSPS

UdA Università degli Studi "G. d'Annunzio"

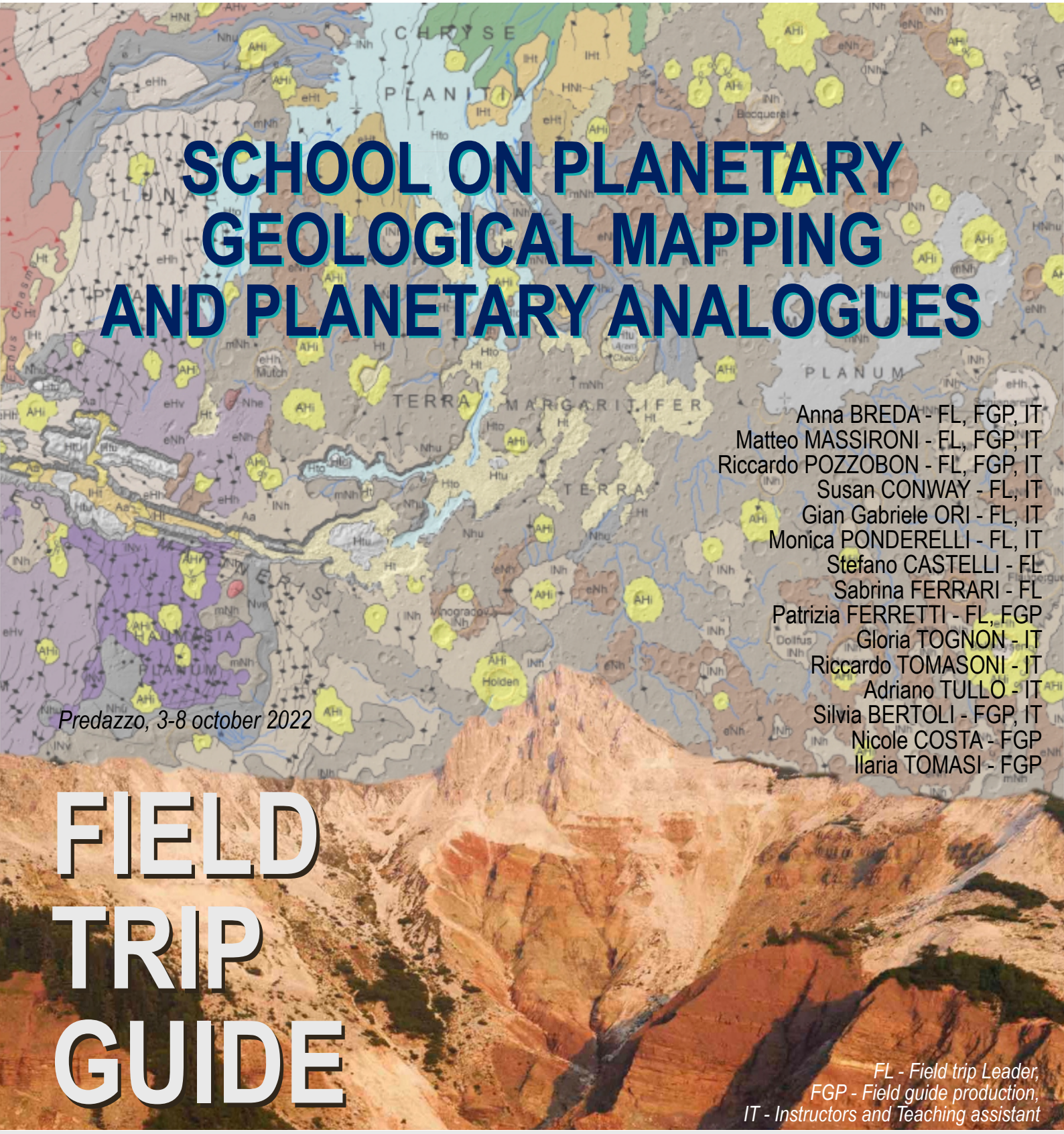

SCHOOL ON PLANETARY GEOLOGICAL MAPPING AND PLANETARY ANALOGUES

Anna BREDA - FL, FGP, IT
Matteo MASSIRONI - FL, FGP, IT
Riccardo POZZOBON - FL, FGP, IT
Susan CONWAY - FL, IT
Gian Gabriele ORI - FL, IT
Monica PONDERELLI - FL, IT
Stefano CASTELLI - FL
Sabrina FERRARI - FL
Patrizia FERRETTI - FL, FGP
Gloria TOGNON - IT
Riccardo TOMASONI - IT
Adriano TULLO - IT
Silvia BERTOLI - FGP, IT
Nicole COSTA - FGP
Ilaria TOMASI - FGP

Predazzo, 3-8 october 2022

FIELD TRIP GUIDE

FL - Field trip Leader,
FGP - Field guide production,
IT - Instructors and Teaching assistant

Dolomiti Dolomiten Dolomites Dolomitis
Fondazione UNESCO

Museo Geologico delle Dolomiti di Predazzo

MUSE La rete dei Musei della Scienza in Trentino

GEOPARC Bletterbach
Aldein • Radein | Aldino • Redagno

Nantes Université

1290 UNIVERSIDADE D COIMBRA

U.PORTO

VR2Planets

Contents

PLANETARY ANALOGUE FIELD GUIDE IN DOLOMITES

Dolomites are widely renowned as a unique geological environment being characterized by well preserved Mesozoic atolls at 2000 m of elevation on average. This peculiar geological character together with the marvellous landscape made up of pale coloured crests and peaks, vertical cliffs, deep valleys and elevated plateaus, make them one of the most attractive mountain range in the world, worth to be inserted among the UNESCO World Heritage list (http://whc.unesco.org/en/list/1237). What is probably less known is that their stratigraphic record of Permian age as well their Quaternary deposits shaped by the action of glaciers and gravity are marvellous examples of Martian analogues.

In particular the Val Gardena Sandstone, which followed an intensive volcanic event of Permian age, represents a semi-arid alluvial plain environment developed along the coast of the Pangaea supercontinent bathed by the east-west gulf branch of Paleo-Tethys ocean in the equatorial region (Massari and Neri, 1997). These Late Permian fluvial red beds interleaved by overbank clays and arid soils, dominated by sulphates nodules and veins, are astonishingly similar to the sedimentary sequences found by the Curiosity in the Gale crater (e.g. Grotzingher et al., 2014, 2015; Nachon et al., 2014; Schwenzer et al., 2016) (Fig.1). Following westward transgression episodes from the Palaeo-Tethys seas triggered the accumulation of shallow marine evaporites (Bellerophon Formation), again a good analogue of sabkha environments on Mars. For these reasons since 2016 the Bletterbach gorge has been chosen as one of the field sites for Astronauts training in field geology by the ESA/PANGAEA course (https://www.esa.int/Science_Exploration/Human_and_Robotic_Exploration/CAVES_and_Pangaea).

On the other hand the paraglacial, periglacial and glacial morphologies and deposits that shaped the Dolomites since the Late Glacial Maximum are perfect examples of comparable environments on Mars where moraines, rock glacier and protalus rampart can be easily found (e.g. Rossi et al. 2011; Hauber et al., 2011; Conway et al. 2018) (Fig.2). Similarly gravitational deposits and morfostructures such talus cones and scree slopes as well as Deep Seated Gravitational Slope Deformations (DSGSD), so common in the Dolomites, found countless examples on Mars (Crosta et al., 2018; Discenza et al., 2021) and other planetary bodies of the Solar System. Finally debris flows, extremely frequent in Dolomites, are among the most reliable interpretations of the Martian gullies (Lanza et al. 2010; Conway et al., 2011, 2018; Johnsson et al. 2014; Dundas et al., 2022) (Fig.2).

Here we propose three field trips focused on the diverse geological analogues of Mars that the Dolomites can offer.

- The first field trip will be exclusively dedicated to the Permian alluvial plains and fluvial channels of the Val Gardena Sandstone wonderfully exposed within the Bletterbach gorge.
- The second one (Passo Rolle and Venegia Valley) will cover a great variety of potential analogues encompassing the sabkha facies of the Late Permian Bellerophon Formation at Rolle Pass, the late glacial and Little Ice Age moraines of the Travignolo Glacier, the paraglacial protalus rampart/rock glacier and deep seated

gravitational slope deformations of the Castellazzo Plateau, and the active taluses and debris flows at the base of the Pale di S. Martino cliffs.

- The San Pellegrino Pass field trip will be exclusively dedicated to glacial and paraglacial morphologies including late glacial moraines, extensive rock glaciers and protalus ramparts, debris flows, scree slopes and talus cones.

During both the Vengia Valley and San Pellegrino Pass field excursions we will take the chances to also describe the Permo-Triassic stratigraphic sequence of the Dolomites, although not strictly related to any analogy with Martian geology.

The following field trips have been largely based on previous significant works although partly revisited under the light of the Martian analogies. In particular, the Bletterbach Gorge field trip is based on the works of Massari et al. (1988); the Rolle Pass and Venegia Valley field description is partly inspired by the notes of the S.Martino geological map at the 1:25.000 scale (Massironi et al., 2006); the San Pellegrino Pass guide is mostly based on the geomorphological map of Carton et al. (2021) and the geological maps of Abbà et al., (2018), both produced at the scale of 1:10.000.

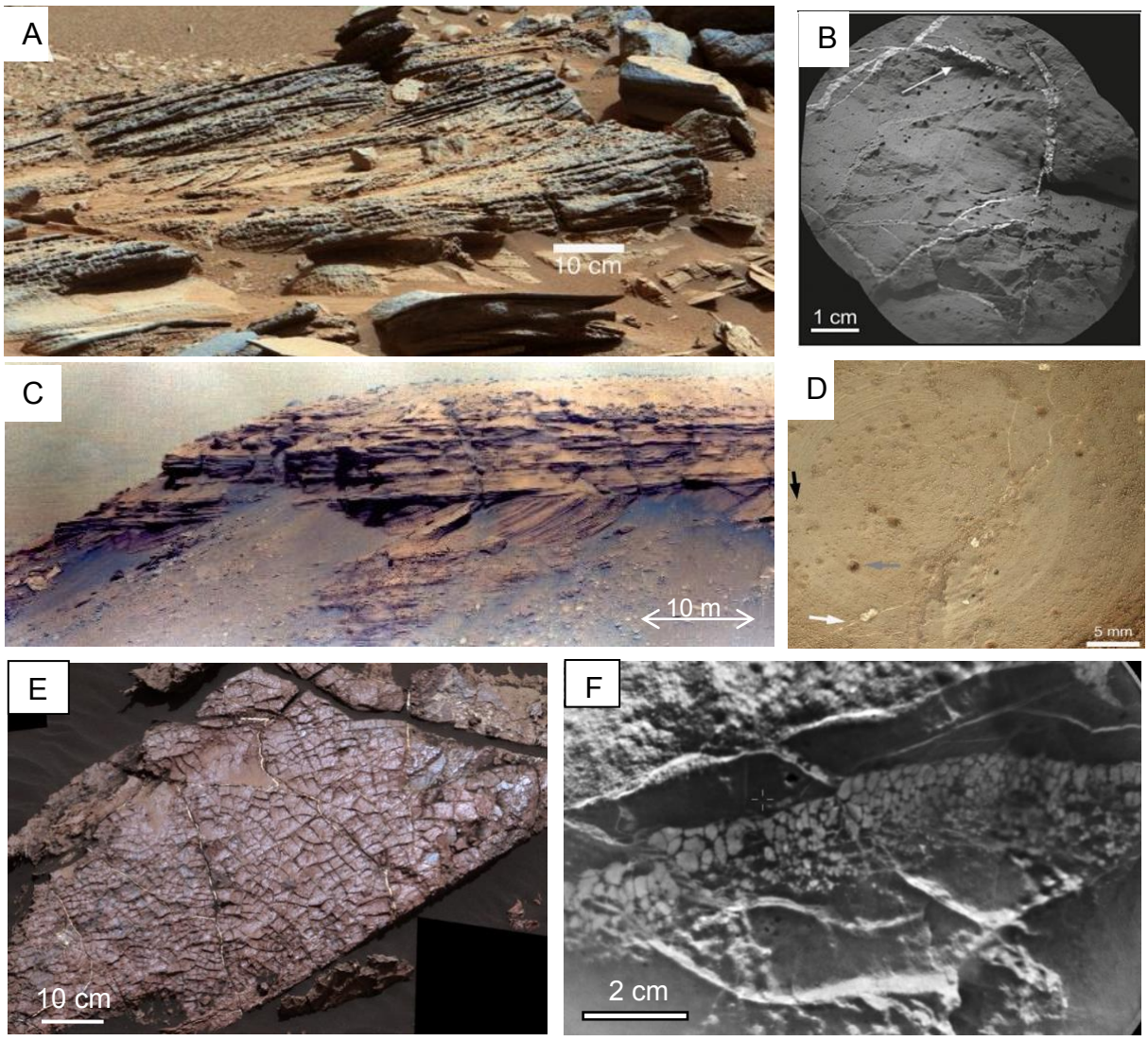

Figure 1 Figure 1. A) Sedimentary rocks of the Yellowknife Bay formation (Gale Crater): Shaler outcrop shows a variety of facies including compound cross-bedding. (Grotzinger et al. 2014), B) Sheepbed target (Gale Crater): white arrow points toward a calcium sulfate vein protruding from the surrounding mudstone (Nachon et al. 2014); C) Cross-stratifications of Kodiak butte (Jezero Crater) (Mangold et al. 2021), D) Mudstone in "Wernecke target" (Gale Crater): nodules (black arrow), void spaces (gray arrow), and sulfate-filled voids can be seen and only those voids connected by hairline fractures (white arrow) have been filled with sulfates (Grotzinger, et al 2014); E) Mud crack and sulphate veins on Old Soaker rock (Gale Crater) Stein et al. 2018,

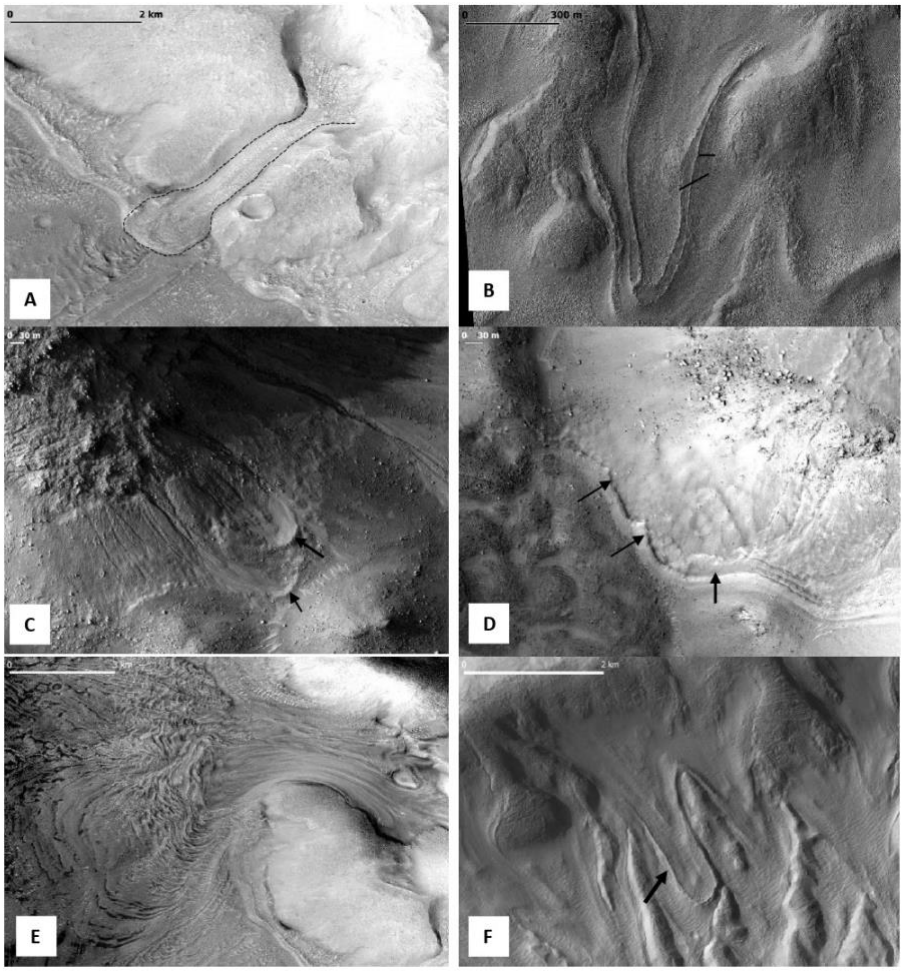

Figure 2 A) Glacier-like features located on the NW rim of Moreux crater. B) A glacier-like flow on north side of crater wall, with latero-frontal moraine ridge. C) and D) Example of protalus ramparts, located on the wall of the central blocks in a floor-fractured crater. E) A complex flow pattern of ice-rich materials that formed multiple lobes resembling rock glacier-like characteristics (Moreux crater). F) The central part of the feature seems to be lowered with respect to its margin, possible indicating a degraded (or "deflated") rock glacier, having experienced a loss of its ice content (unnamed crater, credits by Hauber et al., 2011).

1ST DAY FIELD TRIP: BLETTERBACH GORGE

The main focus of the Bletterbach field trip will be to observe the Upper Permian red beds sedimentary succession spectacularly exposed in the Bletterbach-Butterloch gorge. This gorge near Redagno (Radein) has long been known for its spectacular outcrops and abundance of plant remains and tetrapod footprints (Bernardi et al., 2017; Kustatscher et al., 2017 and references therein).

This succession records alluvial deposition in an arid to highly-seasonal climate and is interested by a variety of sulphate nodules and veins quite similar to those observed in the Gale and Endeavour craters on Mars (Nachon et al., 2014; Crumpler et al., 2015; Schwenzer et al., 2016; de Toffoli et al., 2020).

The Upper Permian red beds belong to the Val Gardena Sandstones unconformably laying on top of the rhyolitic to rhyo-dacitic rocks of the Lower Permian Athesian Volcanic Complex, which is exposed at the base of the Bletterbach gorge. In turn the Val Gardena Sandstone continental deposits transitionally grade into the evaporitic and carbonate deposits of the Bellerophon Formation, clearly showing a general transgressive trend. The whole Val Gardena Sandstone and Bellerophon Formation succession testify an evolution from flashy alluvial fans, through braided-channel bedload rivers, mixed-load sinuous rivers, ephemeral, dryland shallow channels, coastal sabkha and evaporitic lagoon, to shallow, low-gradient shelf. With the only exclusion of the carbonatic shelf all the other environments are perfectly fitting to similar environments documented on Mars (e.g. Grotzingher et al., 2015; Salese et al., 2020; Mangold et al., 2021). For this reason, the field trip will develop only in the lower part of the gorge where the rhyolitic volcanic complex and the red beds are exposed.

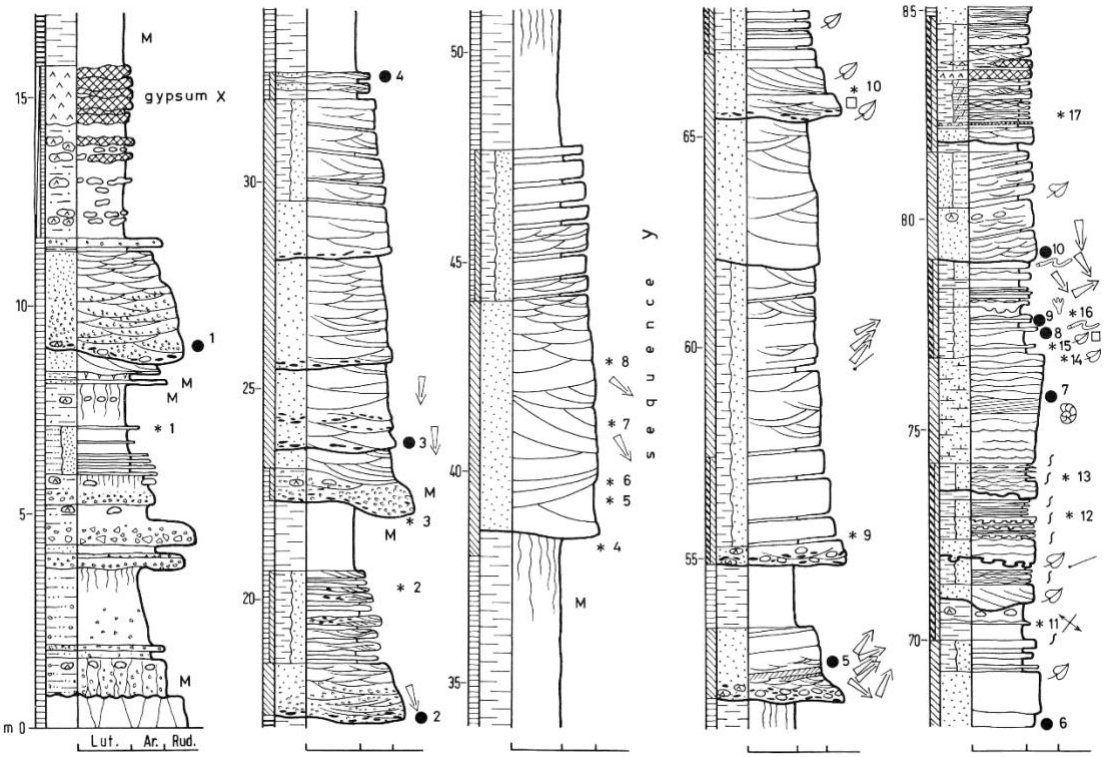

Figure 1.1 Stratigraphic log of the Upper Permian succession cropping out in the Bletterbach gorge (after Massari et al., 1988).

The field trip itinerary and related stops are shown in Appendix 1. in Fig. 1.1, the stratigraphic log of the Val Gardena Sandstone observed during the field trip is shown.

Box "Val Gardena Sandstone facies associations"

Before tackling the description of the stops of the excursion it is worth to describe the main facies associations of the Val Gardena Sandstone in the Bletterbach gorge which can be pivotal examples for interpreting any channelled alluvial plain succession already studied in situ (Grotzingher et al., 2014, 2015; Mangold et al., 2021) or yet to be explored on Mars (e.g. Ori et al., 2000; Fasset and Head, 2005; Pondrelli et al., 2008; Salese et al., 2020).

Bedload river channels

This facies association occurs as composite sandstone bodies resulting from the lateral and vertical amalgamation of channel units (Fig. 1.2) consisting of cross-cutting channels dominated by trough cross-bedded and planar-laminated medium to coarse sandstone. The composite sandstone bodies, typical of braided-rivers, are separated into depositional units by erosive bounding surfaces which make estimates of individual channel depth difficult. Internal architecture suggests deposition in low-sinuosity bedload rivers floored by large three-dimensional dunes, and deposition in a context of low accommodation space.

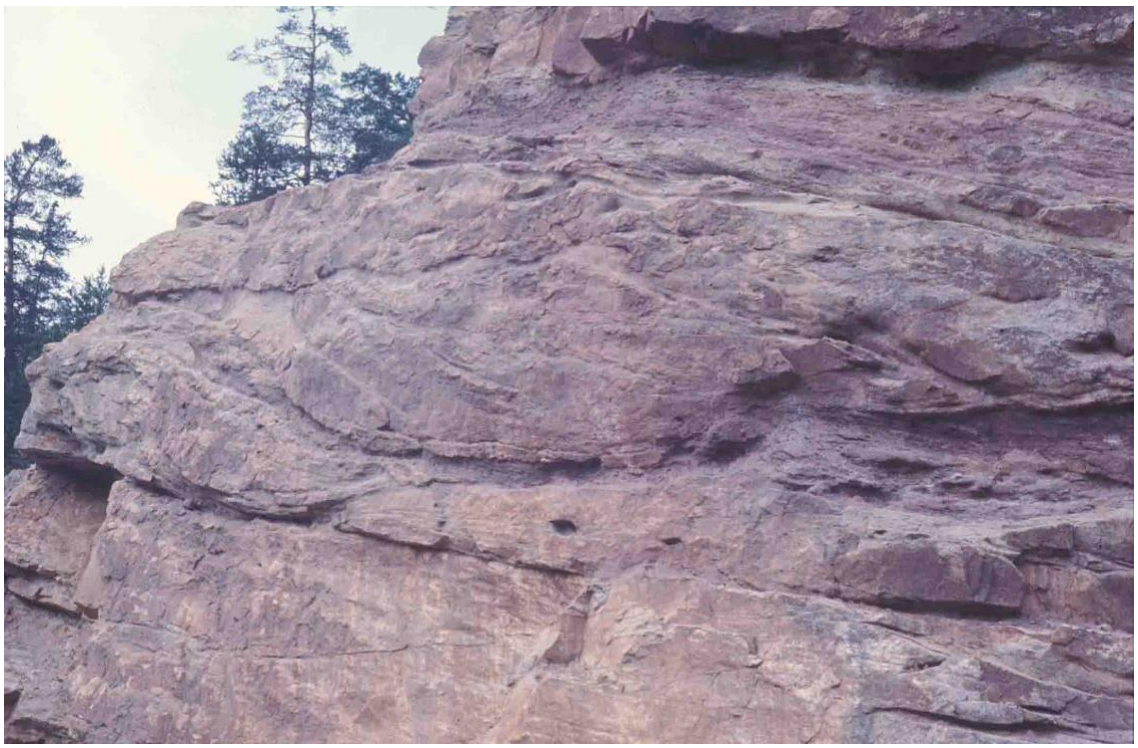

Figure 1.2 Inferred braided-river deposits with evidence of trough cross bedding. Photo: Francesco Massari

Mixed-load channels with evidence of lateral accretion

Tabular channelized bodies with evidence of lateral accretionary pattern are thought to reflect the activity of mixed-load, sinuous channels. Individual channel bodies can be described as point bar sequences and range in thickness from 2 to 10 m (Fig. 1.3). Thicknesses of 9 m or more indicate parent rivers of considerable size, with bankfull depths of the same order of magnitude. The channel fills have low-relief erosional bases, commonly overlain by a patchy coarse lag of intraformational clasts, locally associated with extraformational pebbles, transported plant stems and sometimes tree trunks.

Figure 1.3 Point bar sequence with evidence of lateral accretion and possible chute channel at the top. Photo: Anna Breda.

The lower part usually shows a medium- to large-scale trough cross-bedding and grades upwards into a set of inclined sand/mud interbedding (Inclined Heterolithic Stratification, IHS, of Thomas et al., 1987). Trough cross-bedded sandstone in the lower part of the sequences may have been generated by the flood-stage migration of three-dimensional dunes on the channel floor, or on lower point-bar surfaces. Inclined sand-mud interbedding in the IHS units of some point-bar sequences which grade laterally or vertically to marginal-marine sediments display rhythmic thinner-bedded alternations interpreted as the record of a tidal influence.

Intervals of fine-grained floodplain sediments between sandstone bodies consist of red-brown, structureless, commonly pedogenically modified mudstone (calcrete nodules, mottling, veining, deep polygonal cracks), locally interbedded with sheet-like to broadly lenticular, dm - to - cm sandy layers linked to crevasses or major overbank floods overtopping the channel banks. These occasionally show planar-laminated to ripple-laminated (commonly of the climbing type) waning-flow structures.

Ribbons

Ribbons are generally simple, single-storey lensoid channel fills ranging from 0.9 to 4.3 m in thickness, typically occurring as isolated bodies encased in a significantly high volume of overbank fines, which leads to low channel interconnection (Fig. 1.4). They are characteristic features of the high-accommodation systems tracts.

Ribbons exhibit a sharp, fairly incised, irregular erosional base, sometimes with a remarkably stepped appearance, floored by mudstone clasts and sometimes reworked calcrete nodules and plant debris. Vertically accreted ribbons commonly display a crudely expressed fining-upward sequence, with trough cross-bedding of upward decreasing scale, locally accompanied by planar lamination. In the case of sudden channel abandonment, the channel fill consists of mudstone.

Internal scouring surfaces, in places floored by mudstone clasts, are quite common, and suggest highly fluctuating hydrodynamic conditions. Channel incision occurs after an avulsion event and is commonly followed by one or a number of episodes of plugging and recutting during repetitive flash-flood events.

The ribbons may represent the record of low-gradient, shallow, ephemeral wadi channels prone to frequent avulsion, active with flash-flood regime in semi-arid coastal plains. The scarce persistence of lateral accretionary patterns reflects the lack of sufficient time for lateral channel erosion, due to the ephemeral regime or frequent avulsion (Friend et al., 1986).

Channel fills are interbedded with a great amount of overbank deposits represented by red mudstones and sheet-like splay sandstones deposited by rapid flow into floodplain areas adjacent to the channels during flash floods.

Figure 1.4 Lensoid channel fill (ribbon) overlying a point bar sequence with tabular geometry. Photo: Francesco Massari

The coastal sabkha environment

The inferred transitional setting between the continental environment and the coastal sabkha is characterized by shallow wadi channels and associated splay sandstones merging into mixed flat deposits with weak traces of tidal influence, characterized by flaser- or lenticular-rippled intervals with repeated mud drapes, associated with interbeds of silty dolomicrites with eurytopic microfossils and diffuse bioturbation, and with nodules of chicken wire gypsum forming in the supratidal area.

The typical sabkha cycle consists of three main facies, substantially similar to those described by Bosellini and Hardie (1973):

a) Dm-thick beds of grey marly/silty dolomite, with cm-thick blackish pelitic interbeds. Interpreted environment: low-energy, shallow-subtidal restricted lagoon, similar to the present-day lagoonal setting existing seaward of the Persian Gulf coastal sabkhas (Purser, 1973; Kendall and Warren, 1988).

b) Bedded to massive grey to black marly-silty dolomite with displacive gypsum nodules increasing upwards both in size and abundance. Interpreted environment: intertidal flats at the margin of the supratidal sabkha.

c) Densely packed, layered, nodular gypsum, deriving from facies (b) through further increase in size and abundance of gypsum nodules, which locally coalesce in chicken-wire structures (Fig. 1.5) with the dark marly dolomitic partings reduced to stylolitic undulate seams between gypsum nodules. Interpreted environment: supratidal sabkha, where massive intra-sediment growth of sulphate nodules is continuously fed by solutions rising by capillarity from the water table through evaporative pumping.

Figure 1.5 Sulphate chicken-wire structures in red mudstones. Photo: Anna Breda.

Stop 1 - Lower Permian Athesian Volcanic Complex

In the Latest Palaeozoic, 285–275 Ma, the whole Southern Alpine domain has been affected by a calc-alkaline magmatic activity that produced voluminous basic to acidic volcanic and plutonic rocks (Bargossi et al., 1999 and references therein). In the Trento and Bolzano area the Permian volcanics are termed Athesian Volcanic Complex. The volcanic rocks of the Athesian Volcanic Complex cover in outcrop an area of ~2000 km2 and are topped in unconformity by continental clastic deposits (Val Gardena Sandstone, Upper Permian). The whole thickness of the volcanic sequence is about 2000 m, even though it can be reduced from place to place due to syn-volcanic extensional tectonic activity. Radiometric ages point out that the volcanic activity lasted for 11 Ma, from about 284.9 to 274.1 Ma.

Figure 1.6 The Ora Fm. in the Bletterbach Gorge. Photo: Anna Breda.

Along the Bletterbach Gorge we can see the upper part of the whole volcanic succession locally named Ora Formation, the younger volcanic deposit within the Athesian Volcanic Complex (Fig. 1.6). It is the product of huge volumes of pyroclastic flows. This Formation is made by welded rhyolitic lapilli-tuff, which is very coherent and homogeneous, with a colour ranging from pink-red to orange-red. The rock has a sharp and regular sub-vertical fracturing along two orthogonal sets. The hand-specimen structure is characterised by abundant sanidine, pink plagioclase and quartz crystals (2 - 4 mm), biotite and pyroxene inside a felsitic, fluidal groundmass, which is not homogeneous due to small crystal fragments. Flame structures are frequent and made by dark aphanitic or juvenile porphyric inclusions with the same composition of the rest of the rock. In big outcrops it's possible to observe discontinuity lines, 8-10 m spaced, which cut the rock parallel to the orientation of the fiamme. They could represent the separation of different ignimbrite flow units (Morelli et al., 2007).

Stop 2 - Contact between Lower Permian Volcanic sequence and Upper Permian Val Gardena Sandstone

At this stop it is possible to observe the contact between the Lower Permian rhyolitic Athesian Volcanic Complex and the overlying Upper Permian sedimentary succession composed by the Val Gardena Sandstone and Bellerophon Fm.

A regional unconformity, associated with a time-gap of at least approximately 14 to 27 Ma (Cassinis et al, 1999), and well documented in many places by extensive erosion surfaces and paleosol horizons, marks the passage to the Upper Permian red beds. This interval is consistent with the marked evolutionary changes recorded in the tetrapod footprints of the Southern Alpine Lower and Upper Permian sedimentary deposits (Cassinis et al., 1999). The contact is easily discernible in the landscape, thanks to the different erodibility of the two lithologies (see Figure 1.7).

The local paleotopography covered by the Val Gardena Sandstone is somewhat irregular, leading to slightly variable thickness of the sedimentary cover (Italian IGCP Group 203, 1986). Above a basal regolith of the volcanic substratum, the deposits consist of poorly sorted, matrix-supported conglomerates with angular fragments of rhyolitic rocks, pebbly and muddy sandstones, and siltstones (between 0 and 6m in Fig. 1.1). Finer-grained layers are poorly sorted and consist of a mixture of different proportions of mud, sand and granules; they become better-sorted upsection, where they consist of red to violet mudstones. The coarse-grained layers are apparently unchannelled and may be interpreted as debris flows. They reflect reworking of regoliths and brief transport by mass-flow processes, and may be interpreted as the distal part of a semiarid alluvial-fan (Massari et al., 1988).

Figure 1.7 The transition between the Athesian Volcanic Complex and the Val Gardena Sandstone, as seen from below (A) and from above (B). Note the morphological contrast between the two lithologies. Credits: ESA

Stop 3 - Alluvial-fan to bed-load braided-stream systems

Isolated channel fills 1-2 m thick (Fig. 1.8) and cross-cutting channel complexes up to 9 m thick, composed of laterally coalesced and vertically stacked lenticular sandstones follow up-section (between 9 and 28m in Fig. 1.1), encased in structureless and massive red siltstones, interbedded with sheet-like to broadly-lenticular sparse sandstone beds. Individual channel fills show irregular concave-upward bases, occasionally floored by small to large mudstone clasts, and sometimes fining-upward sequences from pebbly sandstone to siltstone. Trough cross-stratification and horizontal to low-angle cross-lamination are the dominant structures. Interpreted paleochannel geometry, internal structures, and coarse texture indicate deposition in bed-load fluvial channels of shallow to intermediate depths, floored by three-dimensional dunes. The cross-cutting nature of the channel forms in the composite bodies and the lenticular geometry of channel fills point to repeated episodes of channel cutting, sandy infilling and avulsion. The observed features suggest low-sinuosity bed-load braided-stream systems, characterized by high avulsion rate (Massari et al., 1988).

Figure 1.8 Isolated channel fill 2 m thick, encased in structureless and massive red siltstones interbedded with sheet-like to broadly-lenticular thin sandstone beds (between 9 and 11m in Fig. 1.1). Credits: ESA

Gypsum occasionally occurs in the red mudstone in the lower part of the formation (between 12 and 15m in Fig. 1.1), either as sparse nodules clustering along definite horizons or as continuous layers (Fig. 1.9). They are interpreted as components of saline soils (gypcretes) typical of playa basins developing at the toe of alluvial fans. The alluvial fan probably merged into an inland sabkha where high evaporation rates may have caused precipitation of sulphates in the capillary fringe above the water table (Massari et al., 1988). These continental sabkha episodes suggest a splitting of the depositional area into small, isolated, basins during the first stage of the sedimentation of the Val Gardena Sandstone (Italian IGCP Group 203, 1986).

Figure 1.9 Definite horizons of gypsum in the red mudstones in the lower part of the Val Gardena Sandstone (between 12 and 15m in Fig. 1.19b). They are interpreted as components of saline soils (gypcretes) typical of playa basins developing at the toe of alluvial fans. Photo: Anna Breda.

Stop 4 - Alluvial paleosols and sulphate festoon-like structures

Paleosols are abundant along the Bletterbach section, represented by calcic soils, locally with vertic features, which suggest a warm to hot, semi-arid to dry-subhumid climate with strong seasonality (Cassinis et al., 1999). The most common pedogenic features are calcrete profiles consisting of carbonate nodules, mostly developed in red floodplain mudstones with displacive or replacive growth. According to Wopfner and Farrokh (1988), the main carbonate in the nodules of the Val Gardena Sandstone paleosols is dolomite, with magnesian calcite and some magnesite as lesser constituents.

Calcrete profiles are commonly incomplete. As a result of channel scouring, a substantial proportion of them is sharply truncated by an even to slightly irregular surface of erosion. Most immature paleosols are characterized by scattered small nodules showing gradational contacts with the host sediment. More mature soils are characterized by gradual upward increase in nodule size and density, from small and scarce near the base, to larger and partly amalgamated at intermediate levels, to closely packed at the top where they pass into a massive, hard calcrete horizon (hardpan calcrete).

Figure 1.10 Deep cracks crossing red overbank mudstones, are deformed by loading compaction during burial to produce a concertina-like outline. Horizon affected by cracks is about 1 m thick. Photo: Anna Breda.

Where the host sediment is represented by mudstone, the upper part of nodule-bearing profiles is commonly crossed by vertically elongated features typically a few cm wide and up to 2 m deep (between 33 and 39m and between 48 and 51m in Fig. 1.1) (Fig. 1.10) forming a polygonal network in plan. They are most probably deep cracks mainly resulting from repeated expansion and contraction associated with wetting and drying cycles.

Figure 1.11 Festoon-like structures with arcuate fractures sealed with sulphate veins, developing in a paleosol within massive pedogenically-modified overbank mudstones. Both vertical cracks and festoon-like structures are interpreted to result from expansion and contraction associated with repeated wetting and drying of the soil under a seasonally contrasted climate. Photo: Anna Breda.

Definite horizons of gypsum locally appear as festooned structures (Fig. 1.11), with wavelengths of up to 2,5 m, in a few of the massive pedogenically modified overbank mudstone units of the succession. They are defined by gently curved concave-upward intersecting slickensided fractures arranged in conjugate sets. Following Allen (1974), similar features observed in pedogenic carbonate horizons of the Old Red Sandstones, could be compared with the gilgai of certain soils of hot sub-humid to semi-arid regions, produced by the wetting (swelling) and drying (shrinkage) of the deep soil and subsoil. Gilgai (Fig. 1.12) are contorted horizons within soils displaying regularly spaced troughs and ridges created by the seasonal expansion and contraction of soils with high expandable clay content (vertisols) in

response to seasonal variations in moisture (Fitzpatrick et al., 2017; Joeckel et al., 2017; Jewula et al., 2019). Later veins crosscutting the pedogenetic ones and indicating sulphate rimobilization are also observed.

Figure 1.12 Present day gilgai microreliefs in Australia. Source: Fitzpatrick 2015

Stop 5 - The first Upper Permian marine ingression and the Middle Triassic volcanic neck at the waterfall

A distinct fining and thinning upwards trend is observed in the upper part of this interval, resulting from the gradual decrease in thickness and width to depth ratio of channel units. In addition, red overbank mudstones become grey to blackish in colour due to abundance of plant remains and pyrite, suggesting a progressive rise of the water table. Marine influence is heralded in the uppermost part of this interval by the increased intensity of bioturbation and appearance of flaser and wavy bedding, suggesting a tidally-influenced coastal plain (Fig. 1.1, interval between 70 and 74 m). The upward changes in the channel geometry suggest that rivers experienced a progressive decrease in their depth and average discharge in the distal part of their courses, once joined the coastal plain, due to the loss of water by evaporation and infiltration.

This unit, characterized by evidence of marginal-marine setting, is capped by a prominent marine band about 2 m thick (Fig. 1.12), with tabular geometry and a sparse cephalopod fauna which forms a natural step, where the waterfall develops (Bernardi et al., 2018) (Fig. 1.1, interval between 74 and 77m; Fig. 1.39). This marine event, interpreted as a shoreface environment, is uniquely recorded in the Bletterbach gorge, being unknown elsewhere in the Dolomites area and is a puzzling feature whose interpretation and paleogeographical meaning

have been long debated. This band represents the acme of marine influence, and it is interpreted as the inland equivalent of a marine maximum flooding event.

Figure 13. Red overbank mudstones become grey to blackish in colour upwards, due to abundance of plant remains and pyrite, suggesting a progressive rise of the water table. A marginal–marine setting is suggested by the increased intensity of bioturbation and appearance of flaser and wavy bedding, suggesting a tidally-influenced coastal plain. At the top of this interval a prominent marine band with tabular geometry (between 74 and 77 m in the log of Fig. 1.1) forms a natural step in the Bletterbach Gorge. On the right, a volcanic neck is observed crosscutting the sedimentary succession. Photo: Anna Breda.

On the right of the waterfall a volcanic neck infilled with an explosion breccia can be seen crossing the sedimentary succession (Fig. 1.12). This event has been ascribed to the Ladinian, based on the composition of the clasts of the breccia.

2nd DAY FIELD TRIP: ROLLE PASS AND VENEGIA VALLEY

The field trip will give the opportunity to explore the entire Permo-Triassic sedimentary sequence of the Dolomites, although only the Val Gardena Sandstone, the Bellerophon Formation and the Campil member of the Werfen Formation are of interest as Martian analogues.

The sedimentary succession lies on the Lower Permian Athesian Volcanic Complex through a subaerial erosional unconformity (yet visited in the Bletterbach gorge). Above the unconformity stay the Upper Permian alluvial sandstones and siltstones of the Val Gardena Sandstone (AVG), already seen in the Bletterbach Gorge which remains the best exposed location for this environment in the Dolomites. The AVG records deposition in a dryland river system as suggested by the carbonate and sulfate paleosols. The continental succession gradually passes upward to coastal mudflat and sabkha environments pertaining to the Bellerophon Formation (BEL) which are good analogues of similar environments on Mars. These Upper Permian units (AVG and BEL) account for ca. 250 m of sedimentary deposits.

A sharp conformity surface marks the base of the following (mostly lower Triassic) Werfen Formation (Masetti and Neri,1983), a well-bedded continental to shallow marine succession that may achieve a thickness of more than 350 m in this region. The Werfen Formation is subdivided into 9 members with alternating carbonate and siliciclastic lithologies and colors that may vary from gray to greenish, yellow, red and violet.

The Late Anisian to Ladinian sedimentary units rest on the Werfen Formation through an angular unconformity surface overalined by the Anisian Richtofen Conglomerate which is made up of pebbles from the underlying units (Bosellini, 1968). Above, the Anisian succession continues with nodular gray limestones (Morbiac Limestone) and massive white limestones (Contrin Formation) with dasycladacean algae (Masetti and Trombetta, 1998). These three units may attain a maximum thickness of ca. 200 m in the area and on top of them, above a drowning unconformity, is the ca. 600 m thick high-relief microbial carbonate platforms of the Sciliar Formation of which are shaped the Pale di San Martino vertical cliffs. Finally the sedimentary succession is cut by Upper Ladinian mafic sills and dikes, mostly of basaltic composition.

The entire succession was formerly affected by Permian and Mesozoic normal faults roughly North-South trending and afterwards involved in the Alpine orogeny responsible for the formation of ENE thrusts and folds and the strike-slip reactivation of the inherited structures.

Upper Pleistocene glacial deposits pertaining to the Last Glacial Maximum and the Late Glacial in the high Venegia Valley as well as the frontal and lateral moraines of the Travignolo Glacier can be good examples of Martian glacial environments (e.g. Head et al., 2010; Souness et al., 2012; Brough et al., 2016). In addition both the flanks of the Venegia Valley are affected by spectacular Deep Seated Gravitational Slope Deformations (DSGSDs) triggered by the glacial retreat. Due to the different strata attitude on the two flanks of the valley the DSGSDs developed following strikingly different processes: somewhat similar to a megaslide phenomenon in the northern flank, where strata are dipping as the slope, and a lateral spreading to rotational phenomena in the southern flank, where strata dip very gently anti-dip slope. The DSGSDs are indeed common on Mars at the flank

of the Valles Marineris, at the margin of chaotic terrains and in south polar layered deposits (Mege and Bourgeois, 2011; Guallini et al., 2012; Crosta et al., 2018; Discenza et al., 2021).

Protalus rampart/rock glaciers at the base of the Castellazzo mountain are good example of periglacial morphologies found even on Mars (e.g. Conway et al. 2018) whereas the ubiquitous talus deposits laying at the foot of the main rock cliffs are spectacular analogues to similar phenomena visible at the base of any cliffs exposed on planetary or small body surfaces, the most obvious example being the impact craters inner walls.

In Appendix 2 the geological map of the area together with the stratigraphic column, the field trip itinerary and the related stops are shown.

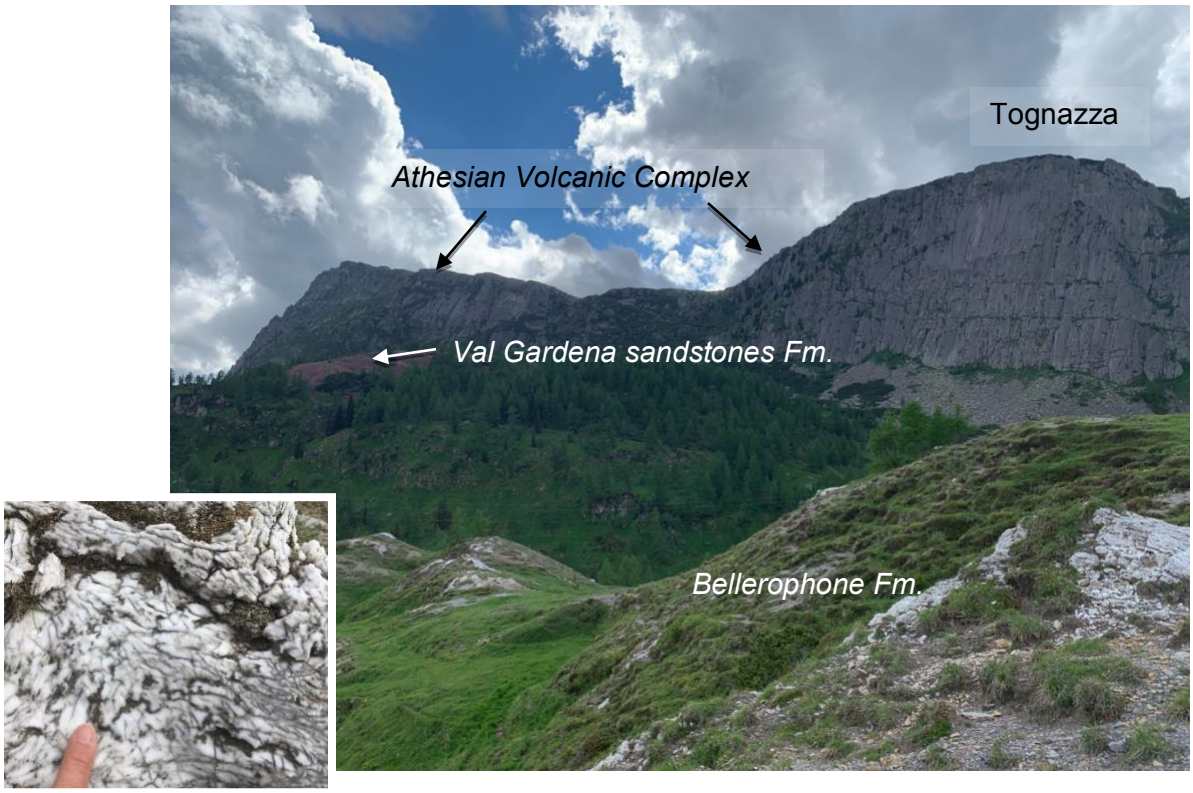

Figure 2.1 Panoramic view of Tognazza cliff from Malga Fosse. In the foreground are the sabkha facies of the Bellerophon formation, in the background the ignimbrites of the Athesian volcanic complex, in between the Val Gardena Sandstones. The units are juxtaposed by normal faults. A fault plane is well visible on Tognazza Cliff (Photo: P. Ferretti). Inset: folded sulfates of the Bellerophon Fm. (Photo: A. Breda)

Stop 1 - Bellerophon Formation and Permo-Mesozoic extensional faulting

The stop is devoted to recognize the typical lithologies of the Upper Permian Bellerophon Formation recording coastal sabkha to evaporative lagoon environments. Most of the succession is characterized by the cyclic alternation of vacuolar and aphanitic dolostones, dolomitic marls, dark clays and laminated gypsum typical of sabkha environments (Fig. 2.1). These lithologies could be potentially analogue to similar Martian environments. However, this succession is highly folded being a weak level of the Dolomitic sedimentary succession and thus an horizon of strain focussing and detachment during the Southern Alpine fold and thrust belt growth. Above the sabkha facies, the uppermost few meters of the Bellerophon Formation is characterized by black and dark limestones rich in marine fauna (brachiopods, calcareous algaes, foraminifera, ostracods, gastropods, bivalves and gastropods between which *Bellerophon* spp.). This facies represents a restricted lagoon environment and is in

turn overlain by the shallow marine deposits of the Werfen Formation. The Bellerophon - Werfen contact coincides with the Permo-Triassic boundary, the most severe extinction event in Earth history, which led to the extinction of more than 80% of marine species and 70% of terrestrial vertebrate species.

In the panorama will be visible the normal faults which bring in lateral contact the Permo-Mesozoic sedimentary series with the Lower Permian Athesian Volcanic Complex. A nice fault plane is well exposed on the up to 150 m high cliff on the eastern flank of the Tognazza Mountain (Fig. 2.1).

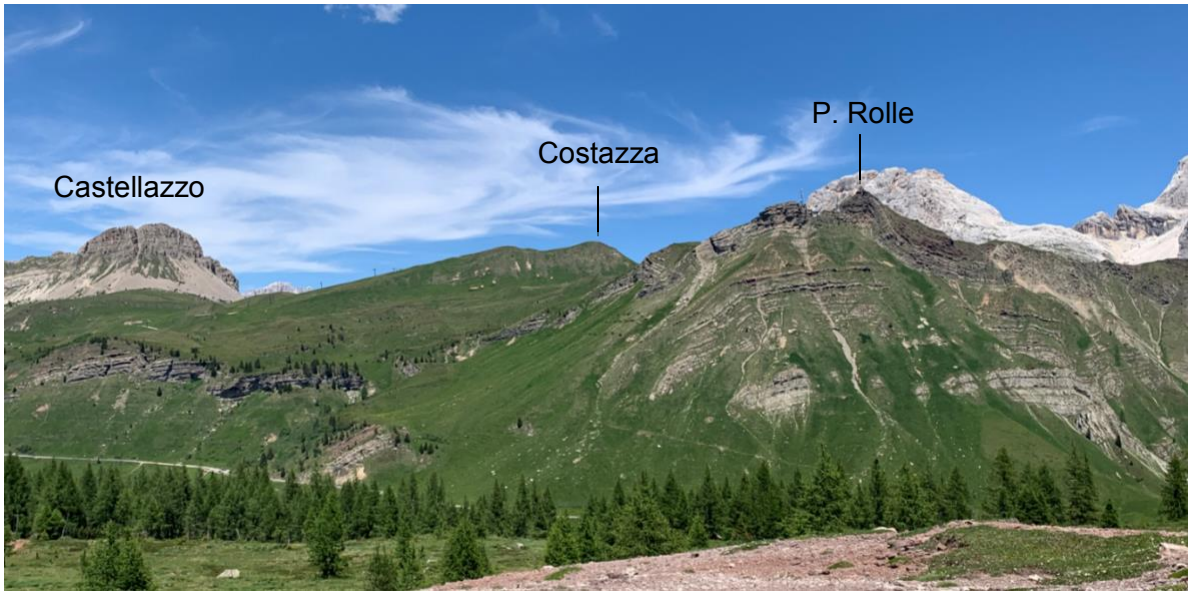

Figure 2.2 Panoramic View of Punta Rolle-Costazza crest looking NE. The landforms are modelled on the Werfen Fm made up of a sequence of carbonate-siliciclastic deposits of different colors indicating a shallow marine succession, in the Background the Anisian carbonatic platform of the Castellazzo mountain (Photo: P. Ferretti).

Stop 2-3-4 - Lower Triassic Werfen Formation

Along the road from Passo Rolle to Baita Segantini the lower members of the Werfen Formation crop out. The Werfen Fm deposited during Early Triassic and records the definitive marine ingression in the Dolomites area and the emplacement of flat shallow marine environments. An alternation of mixed carbonate-siliciclastic deposits reaching a total thickness of about 350 m (when not eroded by the overlying Anisian fluvial Richtofen Conglomerate) is organized in metric to decimetric beds (Fig. 2.2). These facies are not strictly related to any analogy with Martian geology, but present a variety of interesting sedimentary structures that deserve to be observed. In particular the Campil member, widely cropping out along the road and on the Baita Segantini yard, is characterized by decimetric beds of red siltstones and sandstones with abundant load casts, wave ripples, plane-parallel lamination, hummocky cross-stratification, starfish marks, etc (Fig. 2.3). All these structures suggest deposition in a shoreface environment.

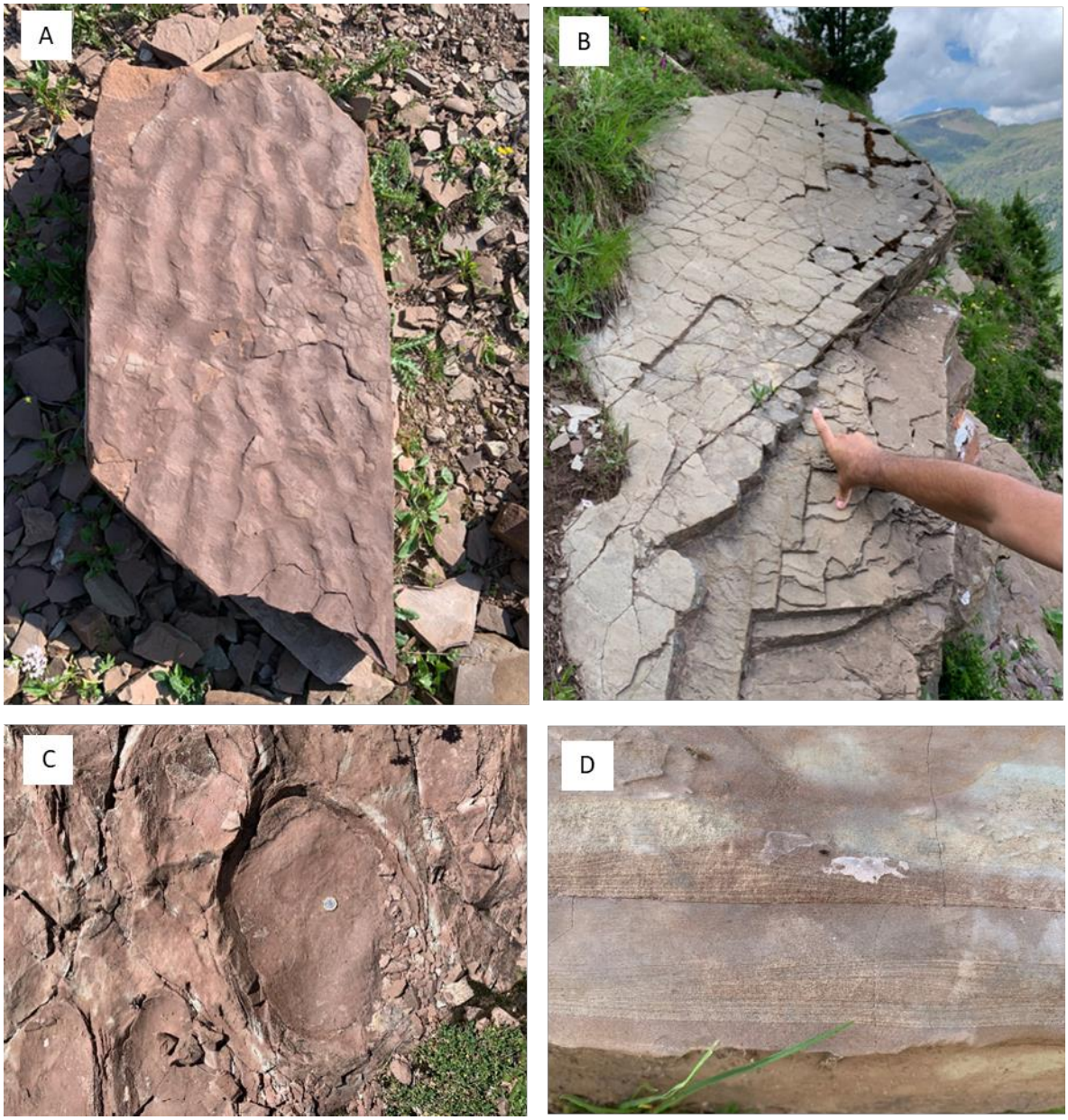

Figure 2.3 Sedimentary structure of the Campil member (Werfen Fm.): A) ripple marks, B) mud cracks, C) load casts, D) cross lamination (Photo: P. Ferretti)

Stop 5 - The Travignolo Glacier and the high Venegia Valley

The panoramic view from Baita Segatini will allow us to appreciate the Quaternary talus deposits of the high Venegia Valley and the glacial ones related to the small Travignolo Glacier. The High Venegia Valley is covered by lodgment till partly covered by debris flow

Figure 2.4 Moraines of the Travignolo Glaciers broken by debris flow gullies and fan (Photo: P. Ferretti).

The Travignolo Glacier is nowadays suffering from a dramatic shrinking which left on its retreat beautiful frontal and lateral moraines. The glacier melting constantly replenishes debris flows which break through the moraines and overlap the glacial deposits within the high Venegia Valley (Fig. 2.4), representing some interesting analogies with Martian gullies.

Close to Baita Segantini is the Costazza hill modelled on siliciclastic members of Werfen formation. These weak lithologies are prone to freeze–thaw induced alteration which generates soliflux lobes similar to lobate features documented on Mars by Johnsson et al. 2012. Marvellous examples are on the Costazza north western slope close to Baita Segantini (Fig. 2.5).

Figure 2.5 Soliflux lobes triggered by freeze–thaw processes on the Costazza north western slope (Photo: P. Ferretti)

Stop 6 - The Castellazzo Mountain: Anisian limestones, Ladininan mafic dikes, protalus rampart and DSGSD

The Castellazzo Mountain rises above the gentle topography produced by the Werfen Fm deposits with a nearly circular ring of vertical cliffs more than 50 m thick and a nearly flat top. This shape is related to the lithological contrast between the Werfen Fm and the overlying Anisian succession. During Anisian, synsedimentary tectonic events led to an important erosive phase and to the consequent deposition of a transgressive succession, recording the transition from continental fluvial conditions (Richtofen Conglomerate) to shallow lagoon environments (Morbiac Limestone) to dasycladaceae bearing carbonate platform (Contrin Formation). The Contrin platform is dissected by extensional synsedimentary faults producing small restricted-circulation basins infilled by dark fine limestones on the bottom and carbonate breccia falling down from the fault scarps (Moena formation) (Masetti and Trombetta, 1998).

The Castellazzo cliffs are shaped on those Anisian limestones and cryogenic processes were responsible of talus deposits underlying their base (Fig. 2.6). Of particular importance in a planetary perspective are the protalus rampart/rock glacier surrounding its south-eastern flank (Fig. 2.7).

The entire north-eastern sector of the Castellazzo mountain is interested by a DSGSD which was triggered by the Glacial retreat in the Venegia Valley and was favoured by the gravitational reactivation of Ladinian mafic dikes. The gravitational collapse can be classified as a complex landslide driven by the lateral spreading of the massive limestones loading the weaker sedimentary sequences of the Werfen Fm and a rotational sliding towards the Venegia Valley. The final result is an articulated gravitational collapse subdivided into at

least three main blocks arranged in a stair-case pattern and separated by huge trenches originated along pre-existing mafic dikes which eased their detachment (Fig.2.6).

Figure 2.6. Castellazzo mountain modelled in Anisian limestones. The base of the cliff is covered by talus deposits whereas its north-eastern slope (on the right) is interested by a DSGSD. The three sliding blocks arranged in a stair case pattern are visible on the right. (Photo: P. Ferretti).

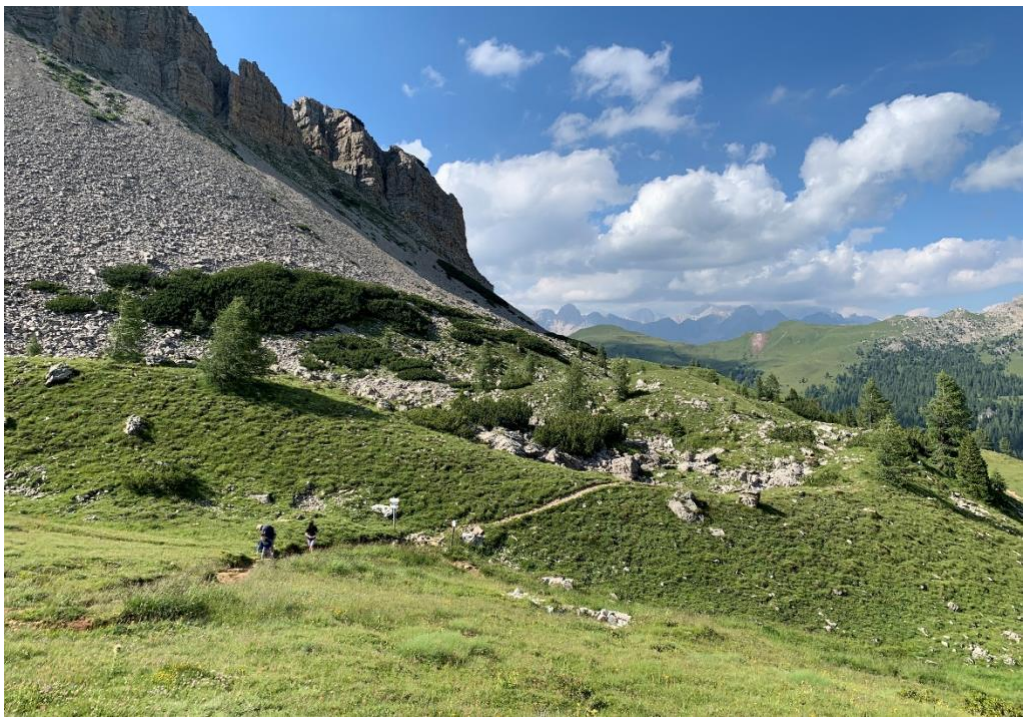

Figure 2.7 Protalus rampart at the base of the Castellazzo south- eastern cliff (Photo: P. Ferretti)

3rd DAY FIELD TRIP: SAN PELLEGRINO PASS

The northern flank of the San Pellegrino Pass area is characterized by the typical landscape of the Dolomites, with high and fairly vertical rock cliffs overlying vegetated slopes and hosting glacial, paraglacial, and gravitational landforms and deposits (Fig. 1). The main focus of the San Pellegrino Pass field trip will be glacial and periglacial processes as well as gravitational deposits, being the exposed bedrock series analogue to the one already described in the Passo Rolle-Venegia valley field trip. The only relevant exception is the upper Ladinian Monzoni pluton in the westernmost sector of the area from which several dikes and sills spread out into the older Permo-Lower Triassic sedimentary sequences giving rise to magnificent examples of morphoselection. Indeed being the mafic dikes more erodible with respect to the Anisian and Ladinian carbonate platforms, they greatly influence the morphology of the ridge where trenches and saddles form in their correspondence often giving rise to debris flow and gullies running downslope.

Although the San Pellegrino Pass area was mostly shaped during the Late Glacial Maximum by the transfluence of a glacier coming from the west (from the Fassa Valley), the most striking glacial and periglacial morphologies and deposits are of Late Glacial period. Those are the ones we propose as well fitting analogues of similar environments on Mars.

In particular the ridge of Costabela Group is carved by several cirques and, at its foot, presents some well-preserved frontal and lateral moraines. These landforms allow to identify five cirques that fed and hosted local independent glaciers, separated by low rocky ridges. The moraines exclusively consist of debris belonging to the local sedimentary rocks and abundant fragments of subvolcanic rocks from dikes and sills of the magmatic complex of Predazzo (Carton et al., 2021).

The deposits of a lake which filled a depression carved by one of these Lateglacial glaciers (Campagnola lake) were dated back to 11,258-11,686 years BP; hence the moraines at the Costabella slope should be attributed to the *Younger Dryas* and a rapid change from glacial to periglacial condition happened in the area during the very early Holocene (Carton et al., 2021). This was the time during which debris-covered glaciers likely evolved into ice-cored rock glaciers (e.g. Berthling, 2011; Seppi et al., 2015). Some of them developed within perimeters previously occupied by the glaciers, while others broke the frontal moraines and moved downslope. They are tongue shaped and characterized by ridges, groves and hollows often disposed in concentric patterns. Three of them are amazing examples of such features and particularly suitable as planetary analogues.

Periglacial conditions are also responsible for the production of frost-shattering debris shaped in the form of protalus ramparts, the main ones visible south of the Selle Pass suggest a transition towards landforms more similar to rock glaciers.

Finally gravitational deposits are recurrent along the steep rock cliffs of the Costabela Group and have produced scree slopes and talus cones. They are mostly active and essentially related to cryogenic processes acting on densely fractured and stratified rocks. Most of them have been intensely modelled by debris flows, which have created large depositional cones and lobes. Presently, on debris flows the linear erosional processes seem to prevail over the

depositional processes, with the formation of deep rills. For this reason these features seem to more faithfully mimic the Martian counterparts.

In Appendix 3 the field trip itinerary and related stops are shown.

Stop 1- Col Margherita panoramic view of the San Pellegrino Pass

Col Margherita rests on an imponent rhyodacite crest pertaining to the Athesian Volcanic Complex and facing the Costabela group bordering to the north the San Pellegrino Pass area. With its 2509 m of elevation is the perfect site to observe the entire sedimentary sequence exposed on the northern slope of the San Pellegrino Pass as well as the great variety of its Quaternary morphologies and deposits (Fig 3.1). The outcropping sequence spans from Lower Permian volcanics of the Athesian Platform to the microbial carbonate platform of the Sciliar Formation of Ladinian age. The sequence is intruded by the Monzoni intrusive complex of upper Ladinian age (here mainly made up of gabbros, monzonites and by the related basaltic dikes). The comparable elevation between the Permian Athesian Volcanic Complex on the San Pellegrino Pass Northern Slope and the Ladinian carbonates on the southern crest is attributed to a triangular structure underneath the glacial deposits of the pass where a south-vergent thrust faces a north-vergent back-thrust, both of Alpine age (Abbà et al., 2018).

The Quaternary deposits are dominated by glacial and periglacial deposits of mostly Holocene age and gravitational debris generated from the Costabela crests.

Figure 3.1 Panoramic view of the south facing slope of the San Pellegrino Pass from Col Margherita. To the left is visible the Triassic intrusion of Predazzzo-Monzone intruding the sedimentary sequence. Pale grey crests and peaks are Sciliar carbontatic platform laying on the Permo-Triassic sequence. The overall panorama is typical of the Dolomites with high subvertical cliffs countoured by talus debris and overlaying vegetated slopes(Credits: Matteo Visintainer – www.geo360.it - tratta da: Geological Landscape. Paesaggio geologico trentino. Tomasoni R. e Visintainer M., Curcu&Genovese, 2018)

Stop 2 - Fuciade hut: Debris and mud flow fans vs talus cones

The Fuciade hut rests on a fluvial scarp margin carved on converging debris and mud flows fans. One of them is still active in its up-slope part and, being close to the talus cones formed by debris falling from Sas da la Tascia cliff (to the northwest), will allow us to make a close comparison between the two morphologies (Fig. 3.2).

Figure 3.2 Debris flow spreading from Sa da Las-cia towards Le Fuciade hut. (Photo: A. Breda)

Stop 3 - Col de le Salae and Val Tegnousa rock glacier

The Col de le Salae is shaped on the evaporites of the Bellerophon Formation and the carbonate-siliciclastic sequence of the lower members of the Werfen Formation, both heavily folded during the Alpine orogen (Abbà et al., 2018). The Col de le Salae can be reached from a narrow east-west oriented valley along which a major alpine south vergent thrust favored water circulation and deposition of important deposits of travertine.

From the degradational scarp carved on Bellerophon Formation just north-west of the Col de le Salae, it is possible a comprehensive view on the Val Tegnousa rock glacier bordering the col de le Salae to the west. With its 2300 m of length it can be considered the most extended and spectacular rock glacier of the Dolomites. It is bordered in the upper part by the lateral moraines of the late Glacial Tegnousa glacier and in the terminal sector it widens, generating a wide steep front resting at an altitude of 1810 m. It is characterized by many ridges, grooves, and close hollows whose interpretation allows us to distinguish different evolutionary phases.

Stop 4 - The Val Fredda rock glacier

Located near Forca Rossa Pass, the Val Fredda rock glacier shows a well preserved morphology whose relationship with the nearby moraine ridges suggest an evolution from a debris-covered glacier (Fig. 3.3). Indeed the rock glacier tongue breaks through the central part of a group of frontal moraines. Part of the rock glacier had been covered by rock fall

debris, which most probably contributed to rock glacier ice core preservation (Carton et al., 2021). Due to its spectacular morphology and “didactic exemplarity” this rock glacier has been included in the list of geosites of the Veneto Region (GV038 - Regional Atlas of Geosites).

Figure 3.3 Frontal lobes of the Val Fredda Rock glacier (Photo: A. Breda)

References

Abbà, T., Breda, A., Massironi, M., Preto, N., Piccin, G., Trentini, T., Bondesan, A., Carton, A., Fontana, A., Mozzi, P., Surian, N., Zanoner, T., Zampieri, D. (2018) Pre-Alpine and Alpine deformation at San Pellegrino pass (Dolomites, Italy). Journal of Maps, volume 14, Issue 2, doi: https://doi.org/10.1080/17445647.2018.1536001

Allen, J.R.L. (1974) Sedimentology of the Old Red Sandstone (Siluro-Devonian) in the Clee Hills area, Shropshire, England. Sedimentary Geology, 12, 73-167.

Bargossi, G.M., Mair, V., Morelli, C., Sapelza, A. (1999) The Athesian Volcanic District (Bolzano-Trento area): a general outline. - In: Cassinis, G. (Ed). Field Trip Book, International field conference on “The continental Permian of the Southern Alps and Sardinia (Italy), Brescia, Italy, 21-24.

Bernardi, M., Petti, F.M., Kustatscher, E.,Franz, M., Hartkopf-Fröder, C., Labandeira, C.C., Wappler, T., van Konijnenburg-van Cittert, J.H.A., Peecook, B.R., Angielczy, K.D. (2017) Late Permian (Lopingian) terrestrial ecosystems: A global comparison with new data from the low-latitude Bletterbach Biota. Earth Science Reviews, 175, 18-43, doi: http://dx.doi.org/10.1016/j.earscirev.2017.10.002

Bernardi, M., Tomasoni, R., Petti, F.M., Kustatscher, E., Nowak, H., Prinoth, H., Roghi, G., Preto, N., Gianolla, P. (2018) Permian–Triassic terrestrial ecosystems of the Dolomites (Southern Alps): Field trip on the occasion of the Paleodays 2018. GeoAlp, 15, 5-36.

Berthling, I. (2011) Beyond confusion: Rock glaciers as cryo-conditioned landforms. Geomorphology, 131, 98-106.

Bosellini, A. (1968) Paleogeologia pre-anisica delle Dolomiti centro-settentrionali. Mem. Atti Acc. naz. Lincei, anno 365 (cl. sc. fis., mat. nat.), ser. 8-9 (sez. 2a): 1-32, Roma.

Bosellini, A. Hardie, L.A. (1973) Depositional theme of a marginal marine evaporite. Sedimentology, 20, 5-27.

Brough, S., Hubbard, B., Hubbard, A. (2016) Former extent of glacier-like forms on Mars. Icarus,274, 37–49. https://doi.org/10.1016/j.icarus.2016.03.006

Carton, A., Abbà, T., Bondesan, A., Fontana, A., Mozzi, P., Surian, N., Zanoner, T., Breda, A., Massironi, M., Preto, N., Zampieri, D. (2021) Geomorphological map of the San Pellegrino Pass (Dolomites, Northeastern Italy). GFDQ – Geografia Fisica e Dinamica Quaternaria. Pages 99-121, suppl. mat. 1-3. DOI 10.4461/GFDQ.2021.44.9

Cassinis, G., Cortesogno, L., Gaggero, L., Massari, F., Neri, C., Nicosia, U., Pittau, P. (1999) Stratigraphy and facies of the Permian deposits between Eastern Lombardy and the Western Dolomites. Field Trip Guidebook. International Field Conference on "The Continental Permian of the Southern Alps and Sardinia (Italy). Regional Reports and General Correlations”, 157pp.

Conway, S. J., Balme, M. R., Murray, J. B., Towner, M. C., Okubo, C. H.,; Grindrod, P. M. (2011) The indication of Martian gully formation processes by slope-area analysis. Geological Society, London, Special Publications, 356 (1), 171–201. https://doi.org/10.1144/SP356.10

Conway, S. J., Butcher, F. E. G., de Haas, T., Deijns, A. A. J., Grindrod, P. M.; Davis, J. M. (2018) Glacial and gully erosion on Mars: A terrestrial perspective. Geomorphology, Vol. 318, pp. 26–57. Elsevier B.V. https://doi.org/10.1016/j.geomorph.2018.05.019

Crosta, G.B.; Frattini, P.; Valbuzzi, E.; De Blasio, F.V. (2018) Introducing a new inventory of large Martian landslides. Earth Sp. Sci. 5, 89-119. doi:10.1002/2017EA000324.

Crumpler, L. S., et al. (2015) Context of ancient aqueous environments on Mars from in situ geologic mapping at Endeavour Crater, J. Geophys. Res. Planets,120, 538–569, doi:10.1002/2014JE004699

De Toffoli, B., Mangold, N., Massironi, M., Zanella, A., Pozzobon, R., le Mouélic, S., L'Haridon, J., Cremonese, G. (2020) Structural analysis of sulfate vein networks in Gale crater (Mars). *Journal of Structural Geology*, *137*. https://doi.org/10.1016/j.jsg.2020.104083

Discenza, M. E., Esposito, C., Komatsu, G.; Miccadei, E. (2021) Large-Scale and Deep-Seated Gravitational Slope Deformations on Mars : A Review. Gosciences 1–19.

Dundas, C. M., Conway, S. J., Cushing, G. E. (2022) Martian gully activity and the gully sediment transport system. Icarus, 386. https://doi.org/10.1016/j.icarus.2022.115133.

Fassett, C. I., Head, III J. W. (2005) Fluvial sedimentary deposits on Mars: Ancient deltas in a crater lake in the Nili Fossae region. Geophys. Res. Lett. 32, L14201.

Fitzpatrick, R.W., Mosley, L.M., Cook, F.J. (2017) Understanding and managing irrigated acid sulfate and salt-affected soils - An handbook for the Lower Murray reclaimed irrigation area. University of Adelaide press, pp. 127, Adelaide, doi: https://doi.org/10.20851/murray-soils

Grotzinger, J. P., et al. (2014) A habital fluvio-lacustrine environment at Yellowknife Bay, Gale Crater, Mars, Science, 343, 14, doi:10.1126/science.124277

Grotzinger, J. P., et al. (2015) Deposition, exhumation, and paleoclimate of an ancient lake deposit, Gale crater, Mars. Science,350, 12,doi:10.1126/science.aac7575

Guallini, L., Brozzetti, F., Marinangeli, L. (2012) Large-scale deformational systems in the South Polar Layered Deposits (Promethei Lingula, Mars): "Soft-sediment" and Deep-Seated Gravitational Slope Deformations Mechanisms. Icarus, 220(2), 821–843. https://doi.org/10.1016/j.icarus.2012.06.023

Hauber et al. (2011). Landscape evolution in Martian mid-latitude regions: Insights from analogous periglacial landforms in Svalbard. Geological Society, London, Special Publications, 356 (1), 111-132.

Head, J.W., Marchant, D.R., Dickson, J.L., Kress, A.M., Baker, D.M. (2010) Northern mid-latitude glaciation inthe Late Amazonian period of Mars: Criteria for the recognition of debris-covered glacier and valley glacier land system deposits. Earth and Planetary Science Letters 294: 306–320.

Italian IGCP-203 Group (ed.) (1986) Permian and Permian-Triassic boundary in the South-Alpine segment of the western Tethys. Field Guide-book. Field Conf. S.G.I.-I.G.C.P. Project 203, Brescia (Italy), July 1986. Tipolit. Comm. Pavese, Pavia, 180 pp.

Jewula, K., Matysik, M., Paszkowski, M., Szulc, J. (2019) The late Triassic development of playa, gilgai floodplain, and fluvial environments from Upper Silesia, southern Poland. Sedimentary Geology, 379, 25-45, doi: https://doi.org/10.1016/j.sedgeo.2018.11.005

Joeckel, R.M., Ludvigson, G.A., Kirkland, J.I. (2017) Lower Cretaceous paleo-Vertisols and sedimentary interrelationships in stacked alluvial sequences, Utah, USA. Sedimentary Geology, 361, 1-24, doi: https://doi.org/10.1016/j.sedgeo.2017.09.009

Johnsson, A., Reiss, D., Hauber, E., Hiesinger, H., & Zanetti, M. (2014). Evidence for very recent melt-water and debris flow activity in gullies in ayoung mid-latitude crater on Mars.Icarus,235,37–54.

Johnsson, A., Reiss, D., Hauber, E., Zanetti, M., Hiesinger, H., Johansson, L., Olvmo, M. (2012). Periglacial mass-wasting landforms on Mars suggestive of transient liquid water in the recent past: Insights from solifluction lobes on Svalbard. Icarus, 218, (1), 489–505. https://doi.org/10.1016/j.icarus.2011.12.021

Kendall, C.G. St. C., Warren, J.K. (1988) Peritidal evaporite and their sedimentary assemblages. In B.C. Schreiber (ed.), Evaporites and hydrocarbons, Columbia University Press, pp. 66-138, New York.

Kustatscher, E., Bernardi, B., Petti, F.M., Franz, F., van Konijnenburg-van Cittert, J.H.A., Kerp, H. (2017) Sea-level changes in the Lopingian (late Permian) of the northwestern Tethys and their effects

on the terrestrial palaeoenvironments, biota and fossil preservation. Global and Planetary Change, 148, 166-180, doi: http://dx.doi.org/10.1016/j.gloplacha.2016.12.006

Lanza, N. L., Meyer, G. A., Okubo, C. H., Newsom, H. E., & Wiens, R. C. (2010). Evidence for debris flow gully formation initiated by shallow subsurface water on Mars.Icarus,205(1), 103–112

Mangold et al. (2021) Perseverance rover reveals an ancient delta-lake system and flood deposits at Jezero crater, Mars. Science 374, 711–717, https://www.science.org/doi/10.1126/science.abl4051

Masetti, D., Trombetta, G.L. (1998) L'eredità anisica nella nascita ed evoluzione delle piattaforme medio-triassiche delle Dolomiti occidentali. Mem. Sc. Geol., 50, 213-237.

Massari, F., Conti, M.A., Fontana, D., Helmold, K., Mariotti, N., Neri, C., Nicosia, U., Ori, G.G., Pasini, M., Pittau, P. (1988) The Val Gardena Sandstone and Bellerophon Formation in the Bletterbach gorge (Alto Adige, Italy): biostratigraphy and sedimentology. Mem. Sc. Geol., 40, 229-273.

Massari, F., Neri, C. (1997) The infill of a supradetachment(?) basin: the continental to shallow-marine Upper Permian succession in the Dolomites and Carnia (Italy). Sedimentary Geology, 110, 181-221.

Massironi, M., Preto, N., Zampieri, D. (2007). Carta geologica della Provincia di Trento scala 1:25000 con note illustrative: Tavola 45 III S.Martino di Castrozza. TRENTO: Provincia Autonoma di Trento, pp. 84.

Mège, D., Bourgeois, O. (2011) Equatorial glaciations on Mars revealed by gravitational

collapse of Valles Marineris wall slopes. Earth Planet. Sci. Lett. 310, 182–191.

Morelli, C., Bargossi, G.M., Mair V., Marocchi M., Moretti, A. (2007) The Lower Permian Volcanics along the Etsh Valley From Meran to Auer (Bozen). Mitt. Österrei. Miner. Ges,. 153, 195-218.

Nachon, M., et al. (2014) Calcium sulfate veins characterized by ChemCam/Curiosity at Gale crater, Mars. Journal of Geophysical Research: Planets, 119 (9), 1991–2016. https://doi.org/10.1002/2013JE004588

Ori, G. G , Marinangeli, L., Baliva, A., (2000) Terraces and Gilbert-type deltas in crater lakes in Ismenius Lacus and Memnonia (Mars). J. Geophys. Res. 105, 17629–17641 (2000).

Pondrelli, M., Rossi, A.P., Marinangeli, L., Hauber, E. , Gwinner, K. , Baliva, A., Di Lorenzo, S. (2008) Evolution and depositional environments of the Eberswalde fan delta, Mars. Icarus, 197, pp. 429-451

Purser, B.H. (1973) The Persian Gulf: Holocene carbonate sedimentation and diagenesis in a shallow epicontinental sea. Springer-Verlag, Berlin, Heidelberg, New York, 471 pp.

Rossi A.P, Van Gasselt S., Pondrelli M., Dohm J., Hauber E., Dumke A., Zegers T., Neukum G. (2011) Evolution of periglacial landforms in the ancient monatin range of Thaumasia Higlands Mars. Geological Society, London, Special Publications, 356 (1), 69–86.

Salese, F., McMahon, W. J., Balme, M. R., Ansan, V., Davis, J. M., Kleinhans, M. G. (2020) Sustained fluvial deposition recorded in Mars' Noachian stratigraphic record. *Nature Communications*, *11*(1). https://doi.org/10.1038/s41467-020-15622-0

Schwenzer, S. P. et al. (2016) Fluids during diagenesis and sulfate vein formation in sediments at Gale crater, Mars. *Meteoritics & Planetary Science*, *51*, 2175–2202. https://doi.org/10.1111/maps.12668

Seppi, R., Zanoner, T., Carton, A., Bondesan, A., Francese, R., Carturan, L., Zumiani, M., Giorgi, M., Ninfo, A. (2015) Current transition from glacial to periglacial processes in the Dolomites (South-Eastern Alps). Geomorphology, 228: 71-86.

Souness, C., Hubbard, B., Milliken, R. E., Quincey, D. (2012) An inventory and population-scale analysis of martian glacier-like forms .Icarus, 217, (1), 243–255. https://doi.org/10.1016/j.icarus.2011.10.020

Stein, N., Grotzinger, J. P., Schieber, J., Mangold, N., Hallet, B., Newsom, H., et al. (2018). Desiccation cracks provide evidence of lakedrying on Mars, Sutton Island Member, Murray Formation, Gale Crater.Geology,46, 515–518.

Thomas, R.G., Smith, D.G., Wood, J.M., Visser, J., Calverley-Range, E.A., Koster, E.H. (1987) Inclined heterolithic stratification-terminology, description, interpretation and significance. Sediment. Geol., 53, 123-179.

Wopfner, H., Farrokh, F. (1988) Palaeosols and heavy mineral distribution in the Groeden Sandstone of the Dolomites. In: G. Cassinis (ed.), Permian and Permian-triassic boundary in the South-alpine segment of the western Tethys and additional regional reports. Mem. Soc. Geol. It., 34 (1986), 161-173.

Appendix 1

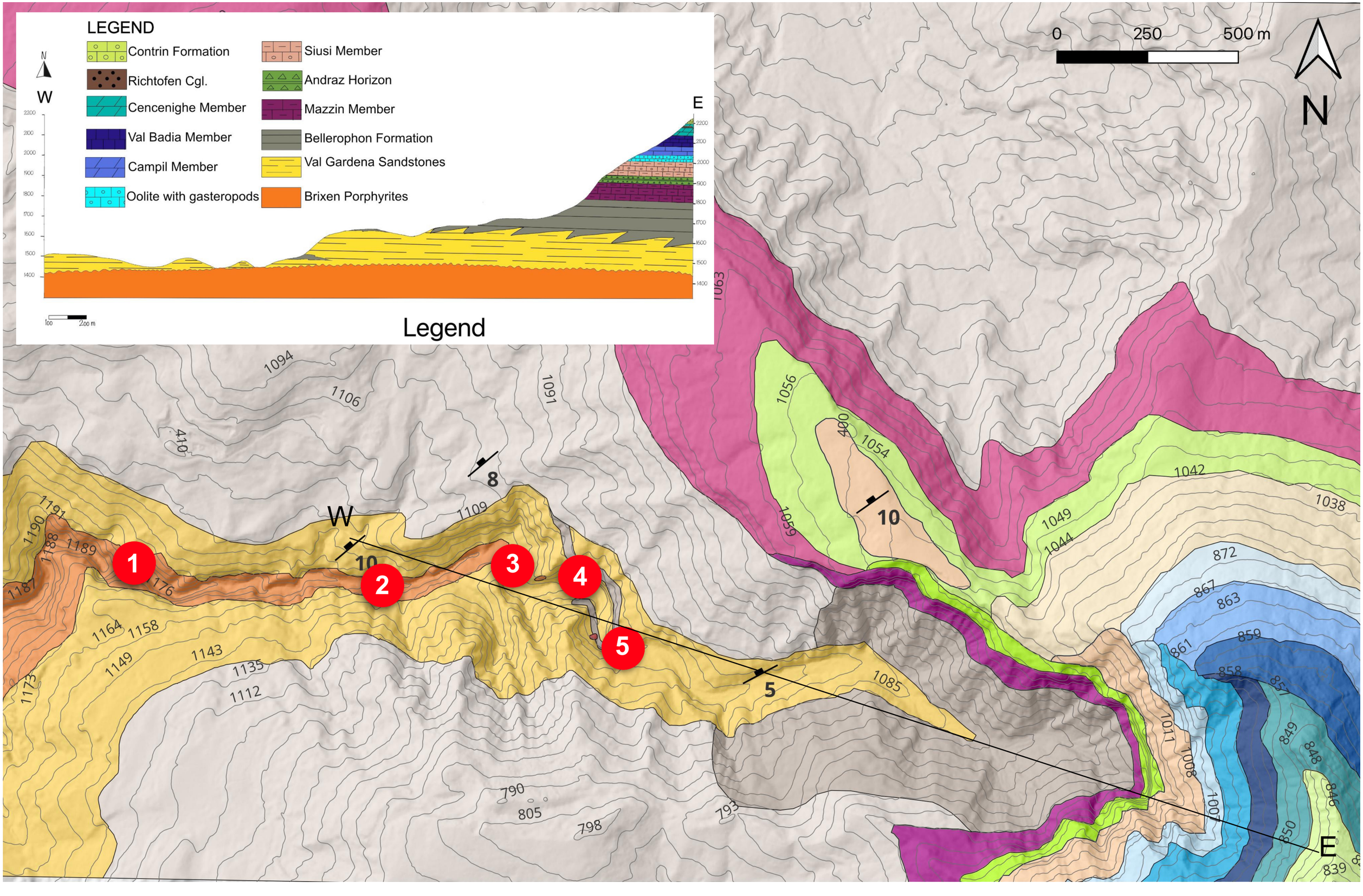
LEGEND
Contrin Formation
Richtofen Cgl.
Cencenighe Member
Val Badia Member
Campil Member
Oolite with gasteropods
Siusi Member
Andraz Horizon
Mazzin Member
Bellerophon Formation
Val Gardena Sandstones
Brixen Porphyrites
N
W
E
2200
2100
2000
1900
1800
1700
1600
1500
1400
100
200 m
Legend
0
250
500 m
N
1094
1106
1091
1063
1056
1054
1059
1042
1049
1044
1038
1109
1191
1190
1188
1189
1187
1176
1164
1158
1149
1143
1135
1112
1173
1085
1011
1008
1007
872
867
863
861
859
858
857
849
848
846
850
839
790
805
798
793
410
400
8
10
10
5
W
E
1
2
3
4
5

Appendix 2

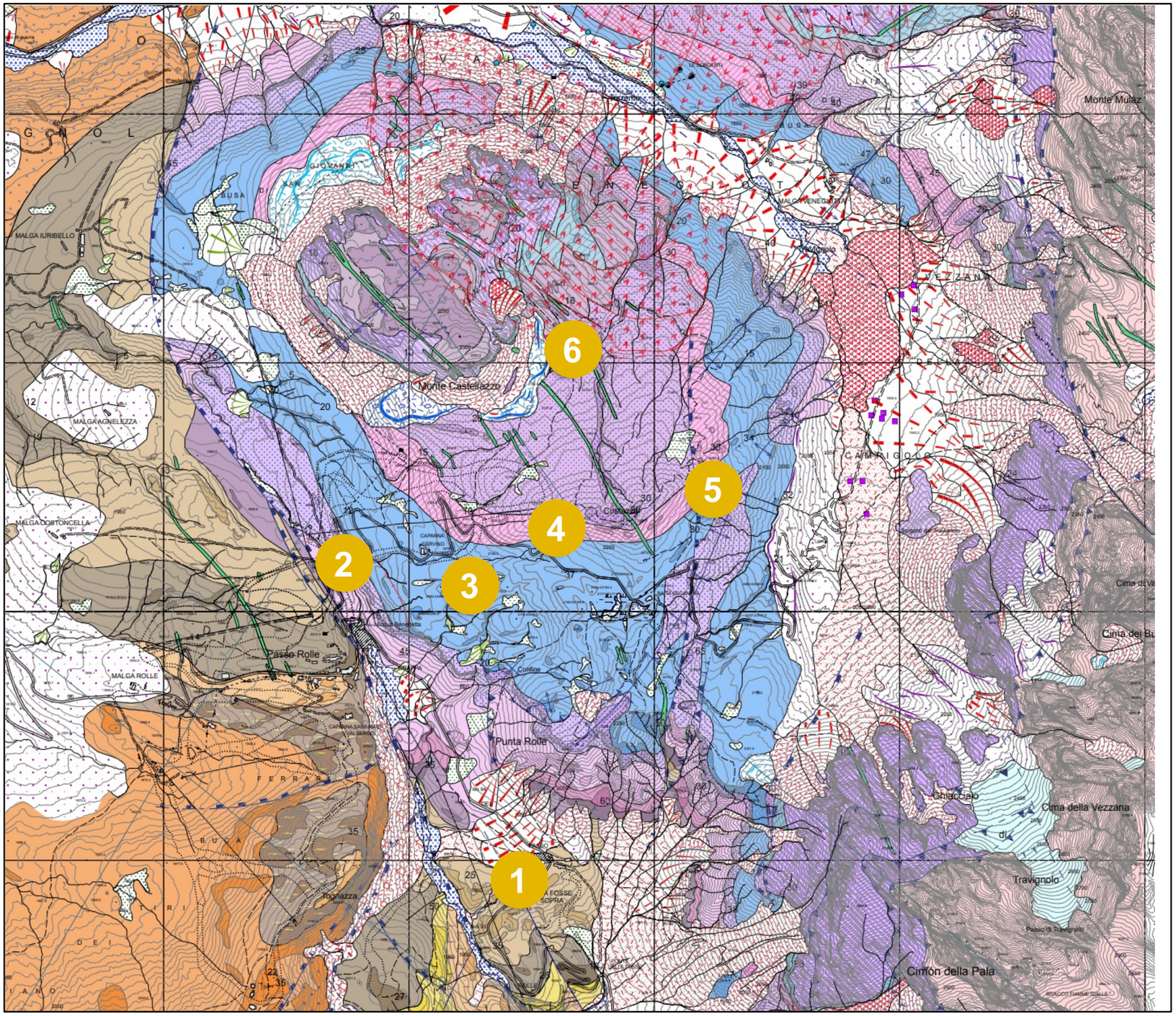

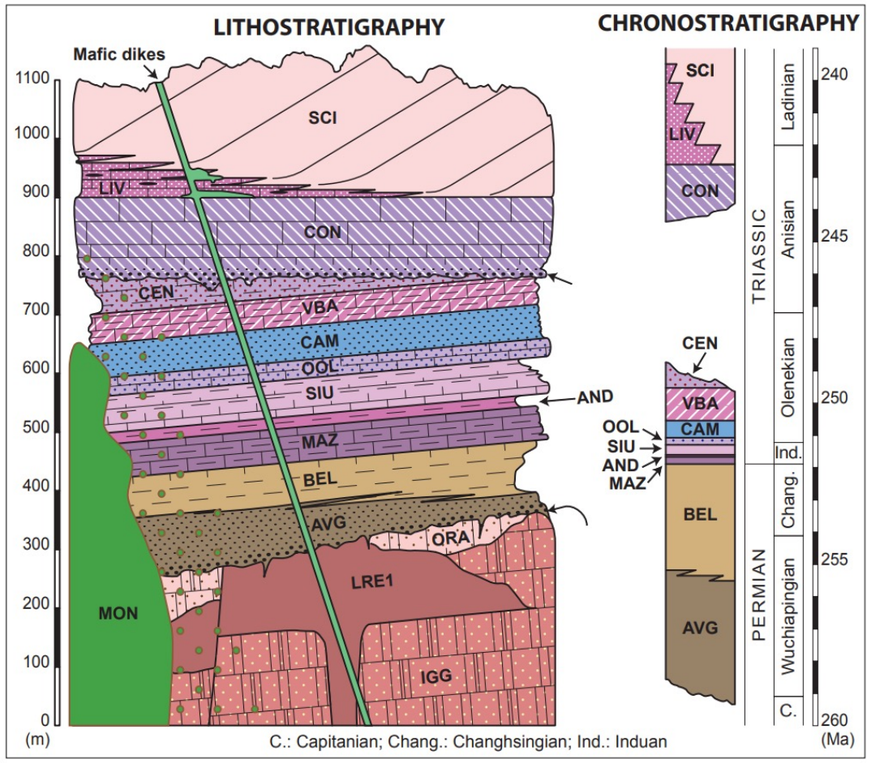

Quaternary deposits

- Talus deposits (a: with large boulders)
- Rock fall deposits
- Earthflow deposits
- Rotational slide deposits
- Indifferentiated till (a: with large boulders)
- Lodgement till
- Rock glacier deposits
- Protalus rampart deposits
- Alluvial deposits (a: cemented)
- Debris-flow deposits
- Palustrine deposits
- Colluvium
- Anthropogenic deposits

Geomorphological features

- Alluvial fan
- Debris-flow fan
- Talus cone
- Colluvial cone
- Moraine ridge
- Protalus rampart ridge
- Rock glacier ridge
- Landslide crown
- Tension crack and trench
- DGPV scarp
- Uphill slope

Structural features

- Strike-slip fault (certain, uncertain)
- Thrust fault (certain, uncertain)
- Generic fault (certain, uncertain)
- Syncline axial plane trace
  Anticline axial plane trace
- Attitude of the beds, with dip angle
- Stratigraphic boundary
- A A' Trace of cross-section

Appendix 3

Scale 1:10.000
0 500 1000 m

Projection: Transvers Mercator
Projection system: ETRS 1989UTM Zone 32N
Datum: ETRS 1989
Spheroid: GRS 1980,6378137.0,298.257222101

Topographic map
Author and owner: Servizio Geologico della Provincia Autonoma di Trento (Italy)
Name: Carta Tecnica 2015
http://www.territorio.provincia.tn.it/portal/server.pt/community/carta_tecnica_provinciale/920/carta_tecnica_provinciale/40052

716000 717000 718000 719000
714000 715000 712000
5145000 5144000 5143000

Cima Cimerlotola · Sforcela del barzavel · Sas de Valfreida · Ponta Ciadine · Pas da le Cirelis · Passo de Strope · Cima dell'Uomo · L'Om · Ponta del Ciadin · Ponta de le Valate · Sas da la Tas-cia · La Bassa del Ciadin · Cima de Costabela · El Cestel de Costabela · Gran Lasté · Cima de Campagnacia · Picol Lasté · Cresta de le Sele · L'Om picol · Col de le Selac · Colifon · 11,258 –11,686 cal BP · Sas dal musc · Lach de le Rizze · Passo di San Pellegrino · MALGA BOCE · MALGA DE COL DE MEZ · Col de mez · Campigol · Blocks · A · B · B'

1 2 3 4

GEOLOGICAL STRUCTURAL FEATURES

BEDROCK

- Mainly limestones (Contrin Fm.,Sciliar Fm.)
- Alternation of limestones and marly limestones with minor siltstones (Mazzin, Siusi, Oolite a Gasteropodi, Val Badia and Cencenighe members of Werfen Fm., Livinallongo (Buchenstein) Fm.)
- Alternation of sandstones and siltstones with minor conglomerates (Campil Member of Werfen Fm., Val Gardena Sandstones, Richthofen Conglomerate)
- Marls, silty marls and siltstones (Bellerophon Fm., Andraz Member of Werfen Fm.)
- Magmatic rocks (Rhyolites of Athesian Volcanic Group; Monzonites, dikes and sills of Predazzo Intrusive Complex)
- Contact metemorphic rocks
- Lithologic boundary
- Boundary between homogenetic morphological units

STRUCTURAL GEOLOGY

- Attitude of the beds (tilted, sub–horizontal) with dip angle
- Fault certain, uncertain
- Thrust certain, uncertain

HYDROGRAPHY

- Spring
- Lake
- Palustrine deposit

STRUCTURAL LANDFORMS

- Edge of scarp
- Structuraly controlled step–slope
- Ridge
- Hogback
- Peak
- Strike–slope

KARST LANDFORMS

- Edge of doline
- Doline or doline field (not in scale)

LANDFORMS AND DEPOSITS DUE TO GRAVITY

active	relict	
		EROSIONAL LANDFORMS
		Landslide crown:
		a) of rock fall
		b) of earth/debris flow
		c) of rotational slide
		Degradational scarp
		Couloir with debris discharge
		Degradational ridge
		CONSTRUCTIONAL LANDFORMS AND DEPOSITS
		Landslide deposit
		Earth flow
		Rotational landslide
		Debris–flow/mud–flowdeposit
		Scree slope
		Talus cone
		Debris–flow/mud–flow fan
		Debris–flow
		Tension cracks/lateral spreading trench

LANDFORMS AND DEPOSITS DUE TO RUNNING WATERS

active	relict	
		EROSIONAL LANDFORMS
		Gully / Barranco
		V–shaped small valley
		Throgh–shaped small valley
		Flat–bottomed small valley
		Incising channel
		Fluvial erosion scarp
		Surface affected by sheet–erosion
		Surface affected by rill–erosion
		CONSTRUCIONAL LANDFORMS AND DEPOSITS
		Stream deposit with texture from boulder to sand
		Conglomerate
		Alluvial fan
		Colluvial deposit
		Colluvial fan

CRYOGENIC AND NIVATION LANDFORMS

active	relict	
		Protalus rampart
		Rock glacier
		Surface with earth hummocks

GLACIAL LANDFORMS AND DEPOSITS

active	relict	
		EROSIONAL LANDFORMS
		Edge of cirque
		Step of trough (Riegel)
		Smoothed surface
		Roche moutonnée
		CONSTRUCTIONAL LANDFORMS AND DEPOSITS
		Morain ridge
		Glacial deposit
		Big boulders glacial deposit
		Erratic boulder

MAN–MADE LANDFORMS

- Excavation surface
- Embankment
- Ski track

GEOCHRONOLOGY

- ^{14}C date

Sample	Depth from lake bottom	Type of material	Radiocarbon age (years BP)	Calibrated age (2σ; cal years BP)
Beta-338312	2.05 m	Plant debris	9400±40	10,510-10,731
Beta-338313	2.55 m	Plant debris	9970±40	11,258-11,686

Radiocarbon dates from core near the center of Campagnola Lake. Age calibrated through the software Calib 8.2(Stuvier et alii, 2021), using the curve IntCal20 (Reimer et alii, 2020).